SLAC-PUB-13117

UCRL-PROC-220696

PRELIMINARY RESULTS FROM THE UCLA/SLAC ULTRA-HIGH GRADIENT CERENKOV WAKEFIELD ACCELERATOR EXPERIMENT

M. C. THOMPSON*, H. BADAKOV, J. B. ROSENZWEIG, G. TRAVISH†

Department of Physics and Astronomy,
University of California, Los Angeles
Los Angeles, CA 90095
E-mail: thompson93@llnl.gov

M. HOGAN‡, R. ISCHEBECK‡, N. KIRBY‡, P. MUGGLI§, A. SCOTT◇, R. SIEMANN‡, D. WALZ‡, R. YODER♦

‡ *Stanford Linear Accelerator Center, Stanford, CA, 94309*
§ *University of Southern California Los Angeles, CA, 90089*
◇ *University of California, Santa Barbara Santa Barbara, CA, 93106*
♦ *Manhattan College Riverdale, NY, 10471*

The first phase of an experiment to study the performance of dielectric Cerenkov wakefield accelerating structures at extremely high gradients in the GV/m range has been completed. This experiment takes advantage of the unique SLAC FFTB electron beam and its demonstrated ultra-short pulse lengths and high currents (e.g., $\sigma_z = 20$ μm at Q = 3 nC). The FFTB electron beam has been successfully focused down and sent through varying lengths of fused silica capillary tubing with two different sizes: ID = 200 μm / OD = 325 μm and ID = 100 μm / OD = 325 μm. The pulse length of the electron beam was varied in the range 20 μm $< \sigma_z <$ 100 μm which produced a range of electric fields between 2 and 20 GV/m at the inner surface of the dielectric tubes. We observed a sharp increase in optical emissions from the capillaries in the middle part of this surface field range which we believe indicates the transition between sustainable field levels and breakdown. If this initial interpretation is correct, the surfaced fields that were sustained equate to on axis accelerating field of several GV/m. In future experiments we plan to collect and measure coherent Cerenkov radiation emitted from the capillary tube to gain more information about the strength of the accelerating fields.

*Current Affiliation: Lawrence Livermore National Laboratory
†Spokesman for the collaboration at Erice.

Contributed to The Physics and Applications of High Brightness Electron Beams, October 9-14, 2005, Erice, Silily, Italy

Work supported in part by US Department of Energy contract DE-AC02-76SF00515

1. INTRODUCTION

The accelerating field achievable in conventional radio frequency accelerators is ultimately limited by the breakdown of the metallic accelerating structure. It is well understood that the field sustainable in a cavity increases with the frequency of the cavity [1,2]. The empirical relation for the surface breakdown field of modern metallic cavities is given by

$$E_s = 220(f[\mathrm{GHz}])^{1/3}\ \mathrm{MV/m}, \tag{1}$$

where f is the RF frequency and E_s is the maximum sustainable surface electric field, which is about 2.5 times greater than the maximum accelerating field [2]. It is difficult to simply follow this scaling by using ever higher frequency cavities due to what could be called the "THz gap"; the current lack of practical high power source between X-band microwaves ($\sim$ 11 GHz) and infrared lasers ($\sim$ 28 THz).

There is considerable interest in the optical limit of break down scaling and the building of dielectric structures powered by high intensity laser beams. Various studies have indicated that GV/m accelerating fields should be possible in dielectric laser accelerators [3] as long as the driving laser pulses are very short [4]. The difficulty with laser accelerators, however, is that they operate at very short wavelengths (e.g. 10.6 μm at 28 THz), which greatly complicates beam injection and phasing.

Dielectric accelerators can also be powered directly by high energy charged particle beams via wakefield excitation [5,6], eliminating the need to generate high power electromagnetic waves. Additionally, a particle beam driven dielectric wakefield accelerator can operate at essentially any wavelength since the accelerating wakefield wavelength is determine by the dielectric geometry. This type of accelerator has been studied in depth over the last several years, but with the maximum fields limited to 10's of MeV/m by the lack of ultra-short drive beams. According to the scaling laws which govern dielectric wakefield accelerators, however, the recently achieved 20 μm pulse-length beams obtained at the Stanford Linear Accelerator Center (SLAC) Final Focus Test Beam (FFTB) facility may be sufficient to generate longitudinal fields in excess of 1 GV/m.

2. THEORY AND SIMULATION

An electron beam driven dielectric wakefield accelerator is essentially an unform dielectric tube coated on the outside with a conductor, see Fig. 1. When an intense electron beam passes through center of the tube its

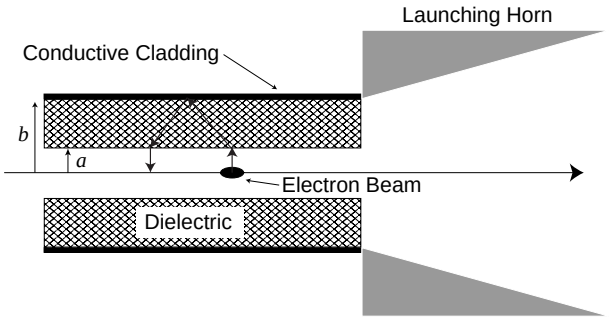

Figure 1. Schematic of the dielectric wake experiment.

electric field bends at the Cerenkov angle within the dielectric, reflects off the outside conducting layer, and returns to the axis where it can be used to accelerate other particles. For an ultra-relativistic beam ($\gamma \gg 1$) it is fairly straightforward to calculate the radial field on the surface of the dielectric $E_{r,surface}$, and the decelerating field within the beam $E_{z,decel}$, to first approximation through simple application of Gauss' law. Such an analysis yields the expression

$$E_{r,surface} = \frac{1}{\epsilon_0} \frac{Q}{(2\pi)^{3/2} a \sigma_z + \frac{\sqrt{\varepsilon - 1}}{\varepsilon} \pi a^2} \left[\frac{\mathrm{V}}{\mathrm{m}}\right], \tag{2}$$

where all quantities are in SI units and Q is the beam charge, a is the inner radius of the dielectric, σ_z is the rms length of the beam, $\epsilon_0 = 8.854$ x 10^{-12} Fm^{-1} is the permittivity of free space, and ε is the dielectric constant. Furthermore, $E_{r,surface}$ and $E_{z,decel}$ are related by the equation

$$E_{z,decel} = \frac{\sqrt{\varepsilon - 1}}{\varepsilon} E_{r,surface}. \tag{3}$$

Table 1. Experiment Design Parameters

Bunch Charge (Q)	3 nC
Bunch Energy	30 GeV
Beam Radius (σ_r)	10 μm
Beam Length (σ_z)	100 - 20 μm
Inner Dielectric Radius (a)	50 and 100 μm
Outer Dielectric Radius (b)	162 μm
Dielectric Relative Permittivity (ε)	~ 3
Peak Decelerating Field	8 GV/m
Peak Accelerating Field	12 GV/m
Peak Field at Dielectric	22 GV/m

By symmetry, it is clear that the accelerating wake behind the driving electron beam $E_{z,accel}$ must be on the order of $E_{z,decel}$, although a more sophisticated analysis is required to predict $E_{z,accel}$ precisely. It is clear from these equations that maximizing the decelerating wakefield, and hence the accelerating wakefield, requires maximizing Q while minimizing σ_z and a. It should be noted that a must be chosen several times larger than σ_r to prevent damage to the dielectric from the beam halo.

The parameters for our experiment, which is based upon the unprecedented combination of high charge, short pulse duration, and small spot size available in the SLAC FFTB beam, are listed in Table 1. The electric field predictions of Eqs. 2 and 3 compare well to those of more rigorous an-

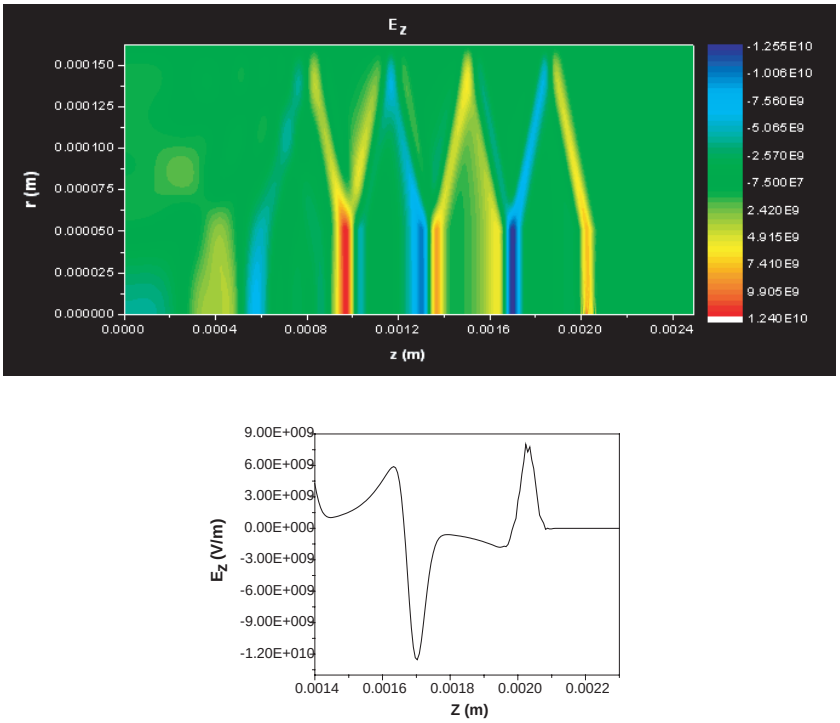

Figure 2. OOPIC simulation results for parameters $Q = 3$ nC, beam energy 30 GeV, $\sigma_r = 10$ μm, $\sigma_z = 20$ μm, $a = 50$ μm, $b = 162$ μm, and $\varepsilon = 3$. At top is a contour plot showing the z component of the electric field (E_z) throughout the simulation region. At bottom is a plot of E_z along the z axis at a radius of 10 μm showing an enlargement of the first wake oscillation. The electron pulse centroid coincides with the peak of E_z on the right.

alytical calculations [8,9] and numerical simulations. Using the values listed in Table 1 and choosing $\sigma_z = 20$ μm and $a = 50$ μm, Eq. 3 predicts a decelerating wakefield within the electron bunch of 8.2 GV/m. OOPIC simulations [10] using the same parameters give a value of 8 GV/m for the peak decelerating field, see Fig. 2. This simulation also indicates a peak accelerating field of 12.5 GV/m, as shown on the right in Fig. 2, and a peak field of 22 GV/m at the surface of the dielectric.

3. BREAKDOWN THRESHOLD OBSERVATIONS

Our experiment is the first in the GV/m regime of electron beam driven dielectric wakefield accelerators. The primary goal of the first phase of the experiment was to assess dielectric material survivability. Since the experiment uses dielectric tubes with 100 and 200 μm IDs, we limited the tube length to about a cm in order to mitigate alignment issues. The energy gained or lost by beam particles was therefore only on the order of 10 MeV, while the full energy spread of the highly compressed FFTB beam is several GeV. Consequently, energy changes were not resolvable in this experiment. The primary signature of high field wakes in this first phase of the experiment was the detection of dielectric breakdown.

This dielectric wakefield experiment is unique in that it produced fields comparable to those in earlier laser breakdown studies. We are particularly interested in differentiating material breakdown in wake-excited, relatively long wavelength (> 50 μm photon) systems, as compared with optically (laser) excited systems. Quantum absorption of photons to produce free electrons in the material is known to be an initiator of avalanche ionization [4]. This mechanism should be mitigated in the wake experiment, since the individual photon energies are lower than in the laser case, perhaps allowing higher fields to be tolerated. In the case of optically excited fields, the breakdown limit for a 70 fs pulse is less than 2 GV/m in fused silica [4]. As discussed below, it seems that surface fields higher than 2 GV/m where sustained in our dielectric wake experiment at similar pulse lengths.

The dielectric tubes for this experiment were modified from off the shelf synthetic fused silica capillary tubing ($\varepsilon \cong 3$), which we procured in 100 and 200 μm ID sizes. Samples were prepared from this bulk product by cutting pieces to length, removing the outer polyimide jacket, polishing the cut ends, and coating the outside of the tube with vapor deposited aluminum. Multiple samples were packaged together for the experiment in a modular mounting block, Figs. 3 and 4. The mounting block is about 1 cm wide, by

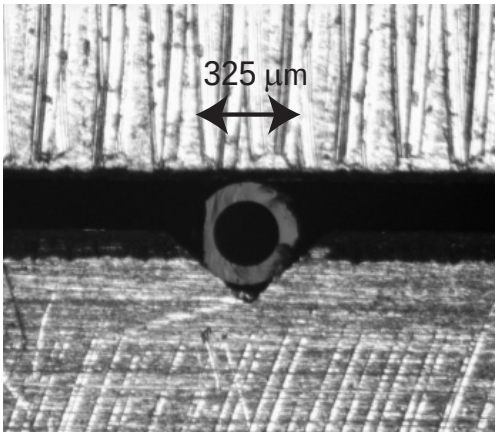

Figure 3. End on view of a 200 μm ID, 325 μm OD capillary tube (unpolished) held in the mounting block.

5 cm long, by 0.5 cm high and is designed to hold 10 samples with 2.5 mm center to center spacing. The mounting block also has an optical transition radiation (OTR) screen for locating the beam orbit and a series of blank alignment holes, as shown in Fig. 4.

Our methodology for aligning the experiment was to move the dielectric tubes onto the established beam orbit rather than trying to steer the beam through the tubes. To accomplish this, the tube sample mounting block was placed on optics mounts and motorized stages to provide all the necessary degrees of freedom. An initial rough alignment was done during the experiment installation with an alignment laser matched to the electron beam orbit. Final alignment began by observing the electron beam on the fiber holder OTR screen with a telescopic camera and an insertable pelicle mirror, see Fig. 4. Once the location of the beam center in the camera field of view was established, the fiber holder could be moved through the fixed camera frame and properly aligned with the established beam position. Before trying to propagate the beam through the fibers, we sent the beam through a series of successively smaller blank alignment holes. By passing the beam through these metal walled "dummy" holes and monitoring x-ray emissions in the accelerator enclosure we planned to ensure that the beam is well aligned and its halo is small enough to fit through the dielectric tube. In practice, this alignment technique seemed to work very well, although we could not rule out beam halo scrapping in the blank holes or dielectric tubes since our only x-ray detector was part of the machine protection sys-

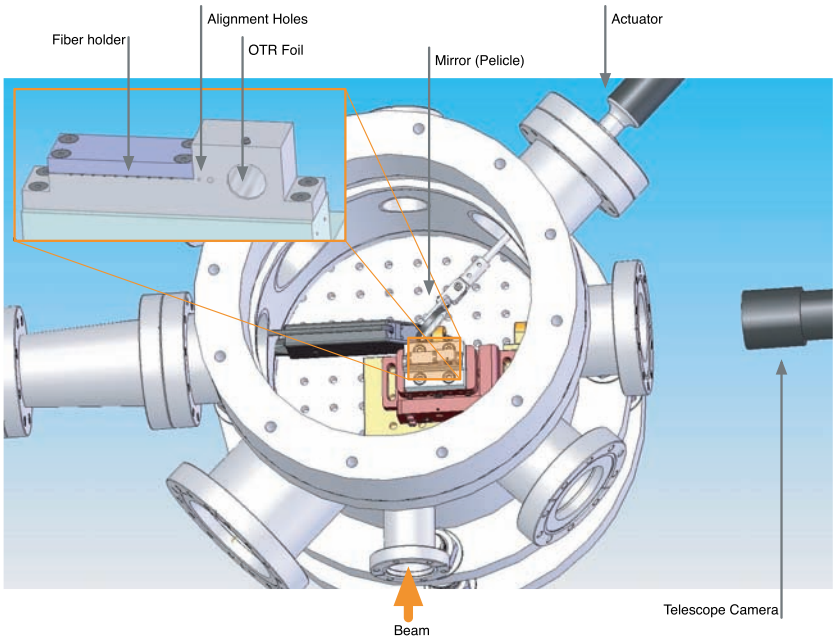

Figure 4. CAD illustration of the experimental setup.

tem and was relatively insensitive. Alignment procedures will be further refined and use better x-ray diagnostics in future runs of the dielectric wake experiment.

Once beam propagation through the dielectric tubes was established, we began to vary the wakefield magnitude by adjusting the beam pulse length and search for an optical signal of breakdown on a side view telescopic camera (not shown in Fig. 4). This experiment was repeated for samples with different tube IDs. Individual tube samples were systematically exposed to different field levels for varying periods of time for a later study of differences in surface damage.

While analysis of the collected data is still preliminary, the observations seem to indicate a clear breakdown threshold. Most of the observations were of 200 μm ID fibers and the general impression is that the visible light output of the fibers jumped up sharply in the middle of the beam pulse length range, Fig. 5. This signal was clearly visible on both the side view telescopic camera and a wide-angle top-view general observation camera. The initiation of breakdown discharges are most likely responsible for the optical radiation increase. The visible wavelength light recorded at

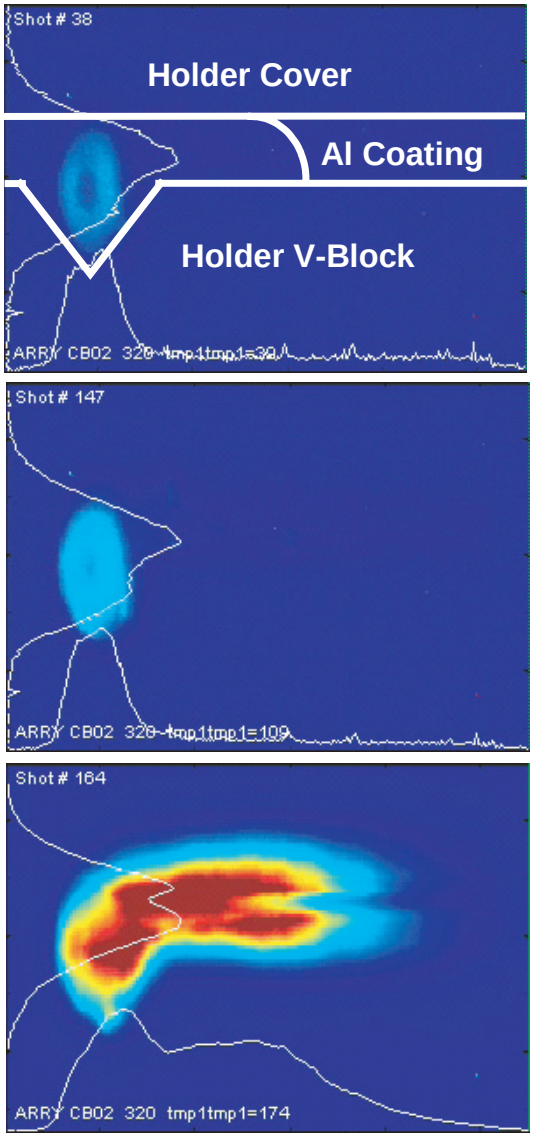

Figure 5. Visible light images (displayed with the same scaled-to-intensity color map) of a 200 μm ID fiber tip as the electron beam pulse current is ramped up. In the top image, the electron beam pulse length is long ($\sim$ 100 μm σ_z) and the fiber end glows faintly with incoherent optical wavelength emissions. The various boundaries of the fiber holder are also illustrated in the top frame, along with the area in which the fiber's aluminum coating blocks optical emissions. In the middle frame the electron beam is shorter and incoherent emission has increased. In the bottom frame the electron beam is near its minimum pulse length ($\sim$ 20 μm σ_z) and a breakdown event has occurred producing a large flash of visible light.

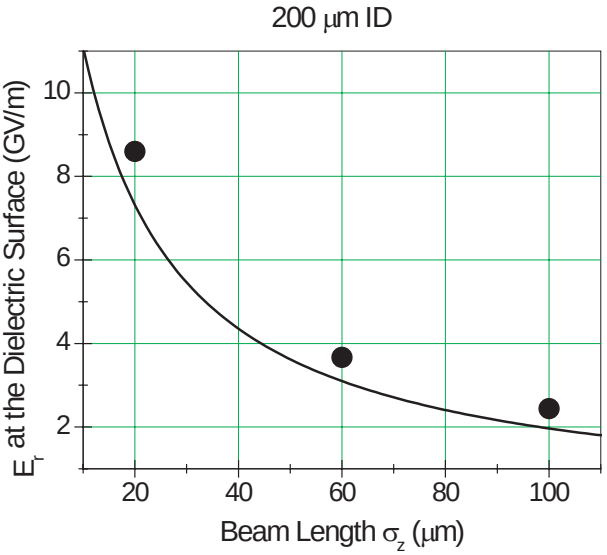

Figure 6. Radial electric field at the inner surface of a 200 μm ID fused silica capillary tube as a function of electron beam pulse length. The line is the prediction of Eq. 2 and the dots are the results of OOPIC simulations. Note that the slight offset arises because the OOPIC results give the peak field while Eq. 2 give the average field over the effective length of the beam. It is not yet clear which method of evaluating the surface fields produces a better figure of merit.

long pulse length / low fields is probably due to a combination of incoherent cerenkov radiation, incoherent transition radiation, and scintillation. Once a breakdown occurs, however, the light from these mechanisms is small compared to the visible emissions from the plasma formed during the breakdown event. It is clear from the observations that breakdown events start to occur after the beam has been compressed below the midpoint of its range. If we plot the surface fields at the dielectric verses the beam pulse length, Fig. 6, we find that at the midpoint ($\sigma_z \sim 60$ μm) the surface fields at the dielectric are in the range 3 - 4 GV/m. OOPIC simulations indicated that this range of surface fields corresponds to 1.5 - 2 GV/m on-axis accelerating fields in the wake.

Further analysis of the data will allow us to make a more accurate determination of the fused silica capillary tube breakdown threshold. In addition to a more careful analysis of the visible light observations and associated beam parameters, we also intend to examine the dielectric tubes with various diagnostics to detect structural damage from the breakdown

events. We hope to be able to correlated the number of breakdown events a particular tube experienced to the degree of pitting or other forms of damage that are evident in the postmortem analysis.

One form of damage which was immediately obvious from cursory examination of the fibers was the vaporization of their aluminum cladding. This type of damage does not impact the study of breakdown, but would be unacceptable in acceleration experiments. When preparing the samples, we assumed that the aluminum coating thickness was unimportant as long as it was substantially thicker than the skin depth at the frequencies of interest. Consequently, we deposited a layer of aluminum about 1 μm thick on the outside of the fibers. After the experiment we discovered that as the number of electron pulses sent through a particular fiber increased, the amount of aluminum remaining on the tube's outer surfaces decreased. We believe that the vaporization of the aluminum resulted from resistive heating of the aluminum cladding due to the electron beam image current. This heating may result in the lose of aluminum through either ablation, long time scale heating of the coating, or a combination of both. In the ablative scenario, each high current beam pulse, which can range from $3 - 18$ kA depending on the pulse length, heats the thin aluminum coating enough to evaporate a small amount of the metal. The temperature of the aluminum cladding would not increase over the long term, however, since residual heat would dissipate between beam pulses. A bulk heating scenario is also possible due to the relative thermal isolation and low mass of the aluminum coating. In this case, as beam pulses travel through the fiber at 1 Hz, the heat deposited by each pulse builds up in the cladding until it is hot enough to sublimate. Initial calculations indicate that significant energy is deposited into the aluminum through resistive heating, but do not resolve which material displacement mechanism dominates. While further work is needed, the vaporization problem can probably be solved in either case by increasing the thickness of the cladding and increasing its thermal contact with the holding block.

4. COHERENT CERENKOV RADIATION

In the second phase of the experiment we plan to measure the quantity and spectral distribution of the coherent Cerenkov radiation (CCR) produced in the dielectric as part of the wake excitation process. An independent measurement of the wakefield strength can be extracted from the CCR properties. The total amount of energy radiated as CCR is approximately

$QE_{z,decel}L_d/2$, where L_d is the dielectric length. This energy is distributed over narrow spectral lines of wavelength $\lambda_n \cong 4(b-a)\sqrt{\varepsilon-1}/n$, where n is an integer, and the energy in each line is approximately proportional to n up to the roll off wavelength $\lambda_n \cong \sqrt{2\pi}\sigma_z$ [7]. For example, using the peak field parameters from Table 1 we find that 150 mJ of CCR will be produced under these conditions with spectral lines at 633, 316, 211, 158, 126, and 106 μm. This THz CCR will have about 5 times the intensity of coherent transition radiation emitted from the surface of the tube end [7]. The CCR will also have a very different spectrum from the coherent transition radiation, which allows for easy differentiation. The CCR exiting the end of the dielectric tube will be collected by an off-axis paraboloid and transported through a vacuum window to a detector. The amount of CCR delivered to the detector will be increased by using a launching horn, similar to those used in microwave antennas, which is just a $\sim 10^\circ$ metal cone placed after the tube exit, see Fig. 1.

5. CONCLUSIONS

We have completed the first phase of a two phase experiment which explores the feasibility of GV/m class Cerenkov wakefield accelerators. The observations of breakdown events made in the first phase of the experiment seem to indicate that a dielectric wakefield accelerating structure based on fused silica can support surface fields of at least 3 - 4 GV/m, which corresponds to accelerating fields of 1.5 - 2 GV/m, without breakdown. These values indicate that a beam driven dielectric accelerator can sustain higher fields, due to its lower photon energy, than a laser driven dielectric accelerator. Further analysis of the data will enable us to refine this initial assessment of the breakdown fields. In the second phase of the experiment we will resolve the problem of aluminum cladding vaporization and measure the coherent Cerenkov radiation emitted by the interaction of the electron beam with the dielectric structure. Analysis of the coherent Cerenkov radiation will give an independent measurement of the strength of the fields within the dielectric.

6. ACKNOWLEDGEMENTS

This work was performed under the auspices of the US Department of Energy under Contract No. DE-FG03-92ER40693 and W-7405-ENG-48.

References

1. W. D. Kilpatrick, *Rev. Sci. Instr.*, **28**, 824 (1957).
2. G. A. Loew and J. W. Wang, "RF Breakdown and Feild Emission", SLAC-PUB-4845 (1989).
3. J. Rosenzweig, A. Murokh, and C. Pellegrini, *Phys. Rev. Lett.*, **74**, 2467 (1995).
4. D. Du, *et al.*, *Appl. Phys. Lett.*, **64**, 3071 (1994).
5. W. Gai, *et al.*, *Phys. Rev. Lett.*, **61**, 2756 (1988).
6. J. G. Power, *et al.*, *Phys. Rev. ST Accel. Beams*, **3**, 101302 (2000).
7. J. B. Rosenzweig, *et al.*, "An Ultra-High Gradient Cerenkov Wakefield Acceleration Experiment at SLAC FFTB," In *Advanced Accelerator Concepts: Eleventh Workshop*, AIP Conf. Proc. No. 737, 811 (2004).
8. R. Siemann and A. Chao, "Wakefields in a Dielectric Tube with Frequency Dependent Dielectric Constant", SLAC ARDB report 368 (2004).
9. R. Siemann, "Decelerating Gradient for FFTB Dielectric Tube Experiment", SLAC ARDB report 371 (2004).
10. D. L. Bruhwiler, *et al.*, *Phys. Rev. ST Accel. Beams*, **4**, 101302 (2001).